ISSN (Print) 1226-1750
ISSN (Online) 2233-6656
Journal of Magnetics 25(3), 341-346 (2020) https://doi.org/10.4283/JMAG.2020.25.3.341

Electromagnetic Analysis of Interior Permanent Magnet Rotor with Dual and Single Layer Magnet Rotor

Chan-Ho Baek[1,2], Chang-Woo Kim[1], and Jang-Young Choi[1]*

[1]*Department of Electrical Engineering, Chungnam National University, Daejeon 34134, Republic of Korea*
[2]*R&D Dept., Hanon-systems, 95, Sinilseo-ro, Daedeok-gu, Daejeon 34325, Republic of Korea*

(Received 25 February 2020, Received in final form 15 July 2020, Accepted 18 July 2020)

This paper proposes a dual layer (delta-shaped) interior permanent magnet rotor with concentrated winding stator for the air conditioner refrigeration compressor of hybrid and pure electric vehicles. The proposed concentrated winding stator design is better than the existing distributed winding stator in terms of the refrigeration vehicle compressor internal flow, light weight structure, and compact design with small end-turn height (thin). However, concentrated winding also has some disadvantages including additional harmonics and torque ripple due to partial saturation. Therefore, this study proposes a design process for a dual layer interior permanent magnet rotor in order to minimize the torque ripple and magnet volume using the finite element method (FEM). The FEM result is determined at the weighted optimum operating point of the electric compressor, and is compared with that of the existing distributed winding model.

Keywords : dual layer IPMSM, optimal design, electromagnetic analysis, T-N curve

1. Introduction

In general, the PMSM structure comprises a distributed winding stator and a surface mounted permanent magnet rotor. This configuration gives sinusoidal electrical characteristics, resulting in convenient and robust control; however, it also has disadvantages such as increased weight and inner wire cooling limitation. Concentrated winding stator can be employed to overcome these disadvantages, namely to achieve direct connection to the load, to improve inner wire cooling, and to ensure a light and compact structure [1-3]. In particular, in the case of an electric motor driven air conditioning refrigerant compressor, the cooling of the electric motor's wire has a big influence on compressor volumetric efficiency [6] and the motor weight also influence electric vehicle driving range. This study proposes a design process for the IPMSM, a lightweight concentrated winding stator through a gas compression load study, and minimizes magnet volume usage and torque ripple through the optimization process of the dual layer interior permanent magnet rotor structure [4, 5]. The motor design process was performed using ANSYS Maxwell's finite element method.

2. Design Target and Process

The design point of IPMSM for electric compressor is determined by operation (speed, torque) point of the compression part in the A/C system of vehicle. The compression torque is equal to the sum of the friction torque of the mechanical parts, the gas load torque, and the acceleration torque. If there is no acceleration torque at steady state and the friction torque is assumed to be constant, the gas torque can be expressed as follows [6]:

$$T_{gas} = \frac{60}{2\pi N_c} \cdot \frac{C_n}{C_n - 1} \cdot P_s v_s \dot{m} \cdot \left[\left(\frac{P_d}{P_s} \right)^{\frac{C_n - 1}{C_n}} - 1 \right] \quad (1)$$

where P_s and v_s are the suction pressure and the suction volume, respectively, P_d and m are the discharge pressure and the mass flow rate, respectively, and N_c and C_n are the compression rpm and the compression index, respectively. As shown in Fig. 1 the operating range of electric driven scroll refrigeration compressor in the A/C systems came from the compression equation (1). These operating points can be summarized in the design specifications of the electric compressor IPMSM in Table 1.

*Corresponding author: Tel: +82-42-821-5651
Fax: +82-42-821-8895, e-mail: choi_jy@cnu.ac.kr

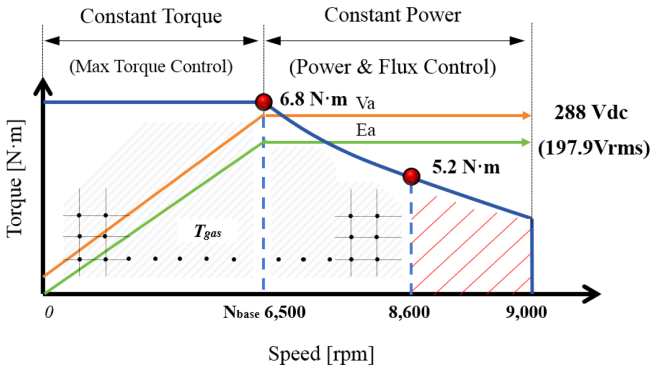

Fig. 1. (Color online) Required operating range of electric driven scroll refrigeration compressor of a vehicle.

Table 1. Specifications of ECOMP IPMSM.

Parameters	Specification	Unit
Battery Voltage (for Motor)	288	Vdc
Rated Power	4.5	kW
Rated Torque	6.8	N·m
Base Speed	6,500	rpm
Max Speed	9,000	rpm

2.1. Concept of dual layer IPMSM

In this paper, the number of 8 poles (600 Hz @ 9,000 rpm) was selected based on the current control frequency of 16 kHz under the same condition as the existing DSP (Digital Signal Process) calculation performance for control the electric compressor. This means that current controller can be calculated 26.67 times at the maximum speed. And an 8-pole rotor structure with 9 slots and 12 slots concentrated winding stator concept can be the selected. But, the harmonic order of the radial pressure is derived from the slots of the stator and the harmonics of the rotor. The stator harmonic is given as $\nu = k\,(S/PP \pm 1)$, where S is the number of slots, PP is the pole pair, and k = 0, 1, 2, ..., and the rotor harmonic component is given as $\mu = (2k \pm 1)$. The 8-pole/9-slot combination can be excluded in compression applications as all orders are represented by radial pressure. Therefore, in this study, the 12 slots configuration was selected. Details of the determination of the pole/slot combinations can be found in several studies [7-9].

The dual-layer IPMSM will be mounted on the same compressor structure as the existing distributed winding stator which can be 96 mm based on compressor O.D. (outer diameter) dimension and internal wall thickness. A rotor O.D. of 60 mm represents a 20 % increase compared with that of the existing distributed winding rotor O.D. (50 mm) in order to account for the increase in the wire fill factor in the stator slot due to concentrated winding. The proposed initial dual-layer rotor used the same magnet material (45SH) and the same silicon steel plate (PN08-35T) as the conventional model. Figure 2 shows a comparison of the single layer and the initial dual layer IPMSM rotor geometries. Table 2 presents the specifications of the interior permanent magnet dimensions and a comparison of magnet size of the existing single-layer 6-pole structure and the proposed dual layer 8-pole structure. The total magnet volume is the almost same as that of a single layer, and the expected performance at the rated operating point (6.8 N·m and 16A) was also achieved.

2.2. Parametric study of dual layer IPMSM

To carry out optimization of the dual layer magnet rotor, the torque ripple was analyzed; In this study, the

Table 2. Comparison of magnet volume.

Rotor Concept (Unit)	M1 (mm)	M2 (mm)	M3 (mm)	No. of Poles	Magnet Volume (mm^3)
Single Rotor Shape	-	19	2.2	6	10282.8
Dual Layer Rotor Shape	8	9	1.2	8	10233.6

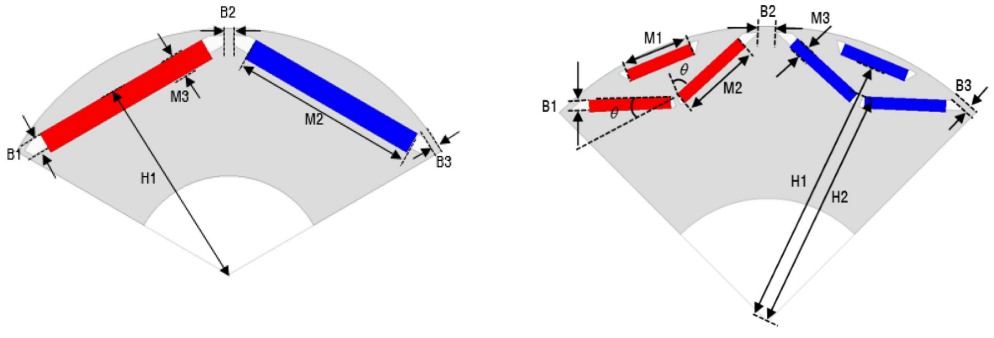

(a) (b)

Fig. 2. (Color online) (a) Existing single layer 6-pole rotor structure. (b) Proposed initial dual layer 8-pole rotor structure.

non-ideal spatial distribution of the flux density in the air gap and the reluctance torque between the permanent magnets and the stator slots was considered. But some issues were not considered, mechanical one such as shaft misalignment and electrical one such as the phase current distortion, fluctuations DC (Direct Current) link from and switching device of dead time [10-12]. Vehicle electric compressor PMSM's out power determined by inverter's input DC voltage and current. The IPMSM input voltage and current equations are as follows:

$$V_{ds}^2 + V_{qs}^2 \le V_{\max}^2,\ I_{ds}^2 + I_{qs}^2 \le I_{\max}^2 \tag{2}$$

Here, V_{ds}, V_{qs}, I_{ds} and I_{qs} are the d-, q- axis terminal voltages and currents, and $V_{\max}$, $I_{\max}$ are maximum DC voltage and current by the inverter, respectively.

The d-, q- axis voltage equations for synchronous reference frame that sets the rotor is rotating at a synchronous speed as standard coordination frame are follows:

$$v_{ds}^e = r_s i_{ds}^e + \frac{d\lambda_{ds}^e}{dt} - \omega_r \lambda_{qs}^e,$$

$$v_{qs}^e = r_s i_{qs}^e + \frac{d\lambda_{qs}^e}{dt} - \omega_r \lambda_{ds}^e \tag{3}$$

in voltage equations (3), d-, q-axis flux component can be present as follows:

$$\lambda_{ds}^e = L_d i_{ds}^e + \psi_f + \lambda_{df\_har},\ \lambda_{qs}^e = L_q i_{qs}^e + \lambda_{qf\_har} \tag{4}$$

Here, λ_{df_har} and λ_{qf_har} are the d-, q-axis interlinked magnetic flux harmonic component caused by the permanent magnet. The torque equation for IPMSM is as follows:

$$T_e = \frac{3P}{4}(\lambda_{ds}^e i_q - \lambda_{qs}^e i_d) \tag{5}$$

The flux equation (4) is substituted into toque equation (5) to obtain equation (6).

Table 3. Dual layer magnet parameters.

	Min (mm)	Max (mm)	Step
H1	22.5	25.5	0.3
H2	29	29.2	0.1
θ(°)	15	30	3
M1	6.2	8	0.2
M2	7.6	8.8	0.2
M3		1.2	

$$T_e = \frac{3P}{4}\{\psi_f i_q + (L_d - L_q) i_a i_q + (\lambda_{df\_har} i_q - \lambda_{qf\_har} i_d)\} \tag{6}$$

Torque ripple component (T_{ripp}) can be derived as in equation (7):

$$T_{ripp} = \frac{3P}{4}(\lambda_{df\_har} i_q - \lambda_{qf\_har} i_d) \tag{7}$$

And the torque ripple percent (%) is defined as follows [13]:

$$T_{ripple}(\%) = \left| \frac{T_{p-p}}{T_{average}} \right| \tag{8}$$

In the vehicle operating conditions, the electric compressor IPMSM has a minimum operating speed of 600 rpm for stable low flow in A/C systems and the maximum speed can be 9,000 rpm due to mechanical stress limitation. And basic operating conditions of vehicle stop conditions is a suction pressure (Ps) of 3 bar (G: Gaged Pressure) and a discharge pressure (Pd) of 12 bar (G) at a driving speed of 3,000~4,000 rpm. The required compression shaft torque in this condition is 3~4 N·m. Therefore, based on this initial requirement conditions, the dual layer permanent magnet parameters can be selected and considered as presented in Fig. 2(b) and Table 3. The row vector explanation of the design parameters (X_{mg}) for dual

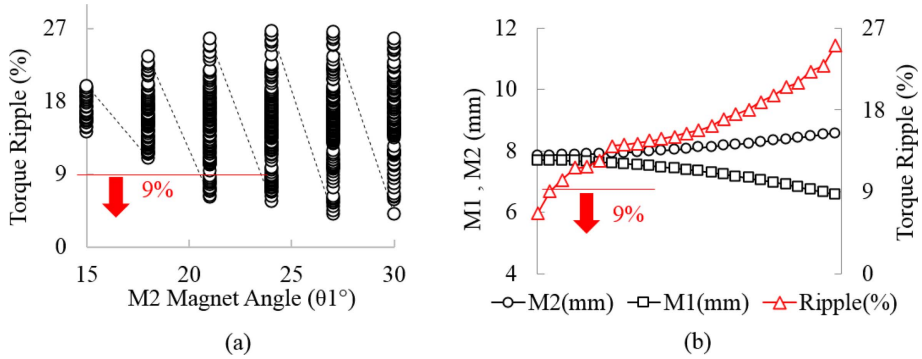

Fig. 3. (Color online) (a) Plot of torque ripple ($T_{p\text{-}p}/T_{average}$ [%]) against the angle (θº) of the dual layer magnet, (b) Torque ripple ($T_{p\text{-}p}/T_{average}$ [%]) along M1 and M2 magnet lengths at the same angle (30º).

layer magnet rotor optimization are represented as follows:

$$X_{\mathrm{Mg}} = [H1\ H2\ \theta\ M1\ M2\ M3]^T \quad (9)$$

From here, H_1 represents the distance from the center of the rotor of the first layer magnet. H_2 is the distance from the center of the rotor at the corner of the second (V-) layer magnet. θ(°) represents the acute angle of the second (V-) layer magnet. M_1 represents the length of the first layer magnet in the dual layer. M_2 represents the length of the second (V-) layer magnet in the dual layer.

2.3. Rotor optimal design of dual layer IPMSM

Table 3 lists the variables that can be considered. The number of rotor geometries that can be generated using Table 3 is 25,740 models. In this study, 758 models were selected into consideration interference between the magnets.

Figure 3(a) show the 758 experimental results under the same input current condition shows that the torque ripple has a periodicity with minimum and maximum values depending on the angle (θ°) of the second layer magnet. Figure 3(b) shows that the increasing of the torque ripple as the difference between the lengths of M1 and M2 increases.

Figure 4. show the following 46 models first select models with less than 9 % torque ripple at the most frequently operating conditions and, dual magnet length same or similar.

Figure 5. show the final model decision process based on the weighting of the driving time (4,000 rpm, 6,500 rpm, 9,000 rpm) it is given in order to consider multiple driving points in the vehicle level. last 6 models are selected among the 46 models, based lowest average torque ripples with weighting point. A comparison of single layer and dual layer models and the final results obtained using the above approach is presented in Table 5.

3. Stator Optimal Design of Dual Layer IPMSM

The stator parameter for the initial concept model is 3 reels of 27 winding turns, as presented in Table 4. This was obtained based on the number of windings of a conventional distributed winding stator design with a slot fill factor of 59.8 %. The proposed concentrated stator winding can be 29 turns of 2 reels based on a similar fill factor 61 %. The stator lamination core length can be reduced from 41 mm to 37 mm by increasing the number of stator wire turns.

Table 4. Stator wire parameters.

Model	No. of Turns	Wire (Coating mm)	Reel	Fill Factor (%)
Initial Concept Model	27	0.75 (0.04)	3	59.8
Opti-Stator #1	28	0.75 (0.04)	3	62.0
Opti-Stator #2	28	0.9 (0.043)	2	58.9
Opti-Stator #3	29	0.9 (0.043)	2	61.0

No.	rpm	M1(mm)	M2(mm)	M3(mm)	θ(°)	H1(mm)	H2(mm)	Vab(rms)	T(Nm)	Tripp(%)
1	4,000	7.8	7.8	1.2	30	22.5	29	110.2509	2.7636	4.11
2	4,000	8	8	1.2	27	24.6	29.1	111.5802	3.0287	4.14
3	4,000	7.8	7.8	1.2	27	24.6	29	109.7002	2.9694	4.55
4	4,000	7.8	8	1.2	27	24.6	29	110.9817	3.0108	5.03
					⋮					⋮
45	4,000	8	8	1.2	21	25.5	29	111.1863	3.0339	8.01
46	4,000	7.6	7.8	1.2	27	24.6	29.1	109.7197	2.9712	8.02

Fig. 4. (Color online) Selected 46 models with less than 9% torque ripple.

	Current Value / Angle						Torque(Nm)			Torque Ripple(%)			Weighting
rpm	4,000		6,500		9,000		4,000	6,500	9,000	4,000	6,500	9,000	3:2:1
1	8.3A	16.3°	16.4A	26°	14.3A	48.1°	3.49	6.85	4.90	5.97	9.72	17.38	9.12
2	8.5A	17°	16.7A	27°	14.9A	47.5°	3.5	6.82	4.91	4.98	9.38	16.67	8.34
3	8.5A	15.5°	16.6A	26.1°	14.5A	48.3°	3.53	6.81	4.91	5.83	10.18	17.74	9.27
4	8.4A	17°	16.5A	26°	14.4A	48°	3.50	6.82	4.92	5.19	10.49	17.42	9.00
5	8.5A	17°	16.5A	26°	14.4A	47.9°	3.53	6.80	4.91	6.25	9.58	16.59	9.08
6	8.3A	16.5°	16.3A	26.3°	14.3A	48.3°	3.51	6.82	4.91	4.94	10.52	18.26	9.02

Fig. 5. (Color online) 6 models from 46 models were selected based on average torque ripple.

4. Model Comparison of Single and Dual Layer Initial and Optimal IPMSM

A comparison of the weighted values (1:2:3) of the critical operating points of the conventional distributed winding motor, the proposed initial dual layer, and the final compact dual layer motor is presented in Table 5. It can be observed that the total length of the laminated core of the final dual layer concentrated winding motor decreased from 41 mm to 37 mm. As a result, the total weight of the motor decreased by 22 %, and the volume of magnet decreased by 11 % (based on the same magnet). The torque ripple weighting value is similar to those of the proposed initial dual layer and the optimized dual layer model. The efficiency weightings are also similar in both designs. Figure 6. show the proto sample of concentrated winding stator and dual layer rotor. Through the demagnetization study, the thickness of the dual magnet was increased to 1.4 mm, and the distance from the center of rotor to the dual layer's magnet were determined to be 23.6 mm. The distance between the first-row magnet and the dual layer magnet is 4.2 mm. The selected first layer magnet length is 7.4 mm and dual layer magnets are 7.8 mm, and the dual magnets angle θ(°) is 24 degrees, respectively. Figure 7. Show the torque ripple comparison between current existing 6 poles single layer rotor and distributed winding type IPMSM and 8 poles dual layer delta shape rotor and concentrated winding IPMSM at rated operation point (6,500 rpm 6.8

Table 5. Single layer and dual layer model comparison.

Stator Core (Length × O.D.)	No. of Turns	Speed (rpm)	T (N·m)	T_{ripple} (%)	T_{Acc_ripp} (%)
41 × 96	12 (108)	4000	3.5	9.57	9.82
		6500	6.8	10.04	
		9000	4.5	10.13	
41 × 96	27 (108)	4000	3.5	4.98	8.34
		6500	6.8	9.38	
		9000	4.5	16.67	
37 × 96	29 (116)	4000	3.5	6.08	8.41
		6500	6.8	8.73	
		9000	4.5	14.74	

Table 6. Single layer and dual layer model weight comparison.

Item	Single Layer Magnet (Distributed winding type)		Dual Layer Magnet (Concentrated winding type)		Density (kg/m^3)
	Volume (mm^3)	Weight (kg)	Volume (mm^3)	Weight (kg)	
Stator	148313.3	1.13	90643.3	0.69	7600
Rotor	48648.1	0.37	65617.9	0.5	7600
Coil	49949.3	0.45	38752.5	0.35	8933
Magnet	9289.0	0.07	8174.3	0.06	7500
Total	256200.0	2.01	204302.5	1.6	

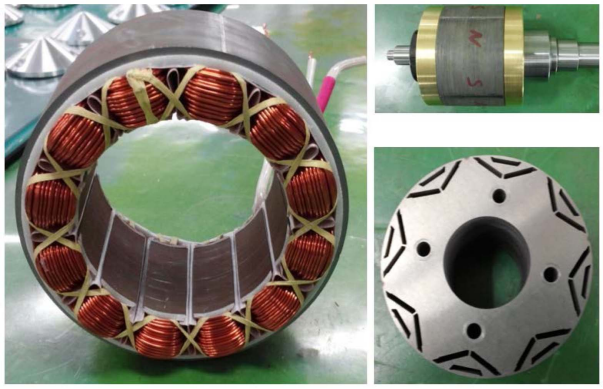

Fig. 6. (Color online) Photographs of concentrated winding stator and dual layer rotor.

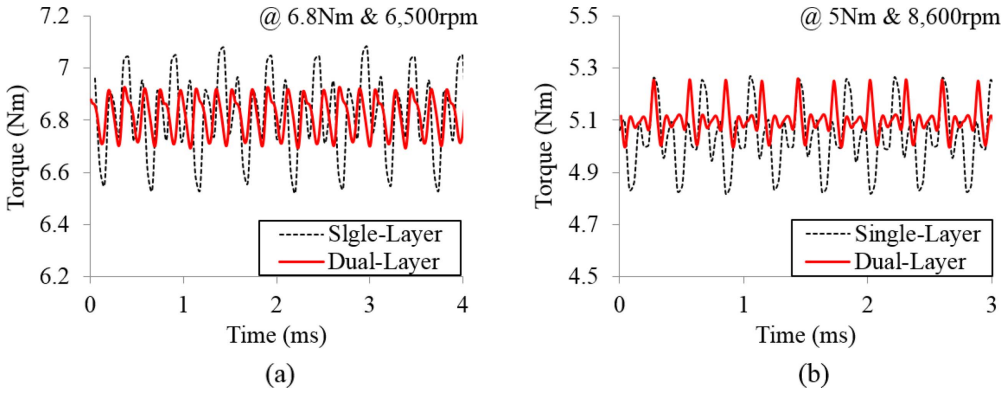

Fig. 7. (Color online) Torque ripple comparison between 6 poles distributed single layer IPMSM and 8 poles concentrated dual layer IPMSM at 6,500 rpm & 8,600 rpm.

N·m and 8,600 rpm 5.0 N·m). Also, it shows single layer IPMSM torque ripple at the this rated operation points about 10 %, dual layer IPMSM about 4~5 %.

As the number of magnets increases from 6 to 16, the cost of magnet maching increases slightly, but it is possible to reduce the material cost by reducing amount of total magnet, wire and stator laminated core through optimal process. The package and weight information are shown in Tables 5 and 6.

Acknowledgement

This work was supported by the National Research Foundation of Korea (NRF) grant funded by the Korea government (MSIT) under Grant 2020R1A2C1007353.

4. Conclusion

This paper describes the overall design process of an electric motor driven air conditioning refrigerant compressor for vehicle. And it shows, the required refrigerant compression torque was calculated from the vehicle's cooling load and the electric motor package decided with internal compressor space limitation. In additionally, it can be referred to the optimization process for minimizing torque ripple with complex magnet inserted rotor shaped structures (a double layer magnet assembly concept) with varying angles as well as distance between magnets. This optimal process considered the weighting values of frequently operating points.

References

[1] S. Vaez-Zadeh, IEEE Trans. Power Electron. **16**, 527 (2001).
[2] E. C. Lovelace, T. M. Jahns, and J. H. Lang, IEEE Trans. Ind. Appl. **36**, 723 (2000).
[3] D. Ishak, Z. Q. Zhu, and D. Howe, In Proc. IEEE Industry Applications Conference **2**, 1055 (2004).
[4] M. Khanchoul, G. Krebs, and C. Marchand, IECON 2011-37th Annual Conference of the IEEE Industrial Electronics Society (2011).
[5] J. Y. Choi, H. I. Park, S. M. Jang, and S. H. Lee, Trans. Korean Inst. Elect. Eng. **60**, 1846 (2011).
[6] Y. Chen, N. P. Halm, E. A. Groll, and J. E. Braun, Int. J. Refrig. **25**, 731 (2002).
[7] Y. H. Kim and Y. S. Kook, IEEE Trans. Energy Convers. **14**, 868 (1999).
[8] Y. S. Chen, Z. Q. Zhu, and D. Howe, IEEE Trans. Magn. **42**, 3395 (2006).
[9] F. Libert and J. Soulard, International Conference on Electrical Machines (ICEM), (2004).
[10] De la Ree, J. and Boules, N. IEEE Trans. Ind. Appl. **25**, 107 (1989).
[11] Y. Yang and S. M. Castano, IEEE Trans. Transp. Electrification **99**, 1 (2016).
[12] S. H. Han and T. M. Jahns IEEE Trans. Ind. Appl. **42**, 558 (2007).
[13] Aimeng Wang, Yihua Jia and W. L. Soong, IEEE Trans. Magn. **47**, 3606 (2011).